GEOLOGICA CARPATHICA, 2026, 77, 4, 291–306 https://doi.org/10.31577/GeolCarp.2026.15

Trace element composition and U–Pb ages of detrital rutiles from the Jurassic Sandstones (Bayırköy Formation) in the western Sakarya Zone, NW Türkiye: Provenance constraints of the Bayırköy Formation

FIRAT ŞENGÜN[1,✉] and REGINA MERTZ-KRAUS[2]

[1]Department of Mining and Mineral Extraction, Çan Vocational College, Çanakkale Onsekiz Mart University, 17400, Çanakkale, Türkiye
[2]Institut für Geowissenschaften, Johannes Gutenberg Universitat, Johann-Joachim-Becher-Weg 21, 55128 Mainz, Germany

(Manuscript received February 8, 2026; accepted in revised form May 25, 2026; Associate Editor: Igor Broska)

Abstract: Trace element geochemical and LA-ICP-MS U–Pb data of detrital rutile grains from Jurassic sandstones of the Bayırköy Formation exposed in the western part of the Sakarya Zone were presented to characterize and differentiate potential source lithologies. The Bayırköy Formation commence with coarse-grained conglomerate at the bottom and passes up to medium to coarse-grained sandstone. Fine-grained marl occurs on top of the Bayırköy Formation. This uppermost level of the Bayırköy Formation is separated as nodular limy levels, clayey and marly nodular levels. The Jurassic Bayırköy Formation in northwestern Türkiye was deposited in a mixed continental–marine setting, reflecting the transition from fluvial–deltaic systems into shallow marine environments. The Jurassic sandstones are yellowish brown-colored, medium to coarse-grained and well-bedded, which exhibits shoreface to tidal flat facies suggesting a coastal transition zone with tidal influence. The Nb and Cr contents in rutile grains are in the range of 40–11900 µg/g and 6–5700 µg/g, respectively. According to the Cr–Nb discrimination, the great majority of detrital rutile grains (70 %) are sourced from metapelitic rocks such as mica schists and paragneisses, the rest of detrital rutile grains (30 %) are derived from metamafic rocks such as amphibolites, eclogites and metagabbros. Trace element composition of detrital rutile grains demonstrate that the source rock lithology is predominantly metapelitic in origin. The Zr-in-rutile temperatures range from 480 °C to 790 °C, which indicates amphibolite-facies metamorphic conditions. The U–Pb age data of detrital rutile grains range from 313 Ma (n=72, MSWD=2.6) to 330 Ma (n=53, MSWD=2.5), which yields the age of metamorphism for the potential source rocks of detrital rutile grains in the Sakarya Zone. Trace element composition, Zr-in-rutile temperatures and rutile U–Pb age data exhibit potentially derivation from metamorphic source rocks which underwent metamorphism in amphibolite-facies conditions during Early Carboniferous. Exposures with Variscan amphibolite-facies metamorphic basement rocks can be assumed as likely sources for these sandstones in the Jurassic Bayırköy Formation. Amphibolite-facies metamorphic rocks in the Sakarya Zone seem to be the primary source lithologies for the detrital rutiles in the Jurassic sandstones. Another conceivable source for detrital rutile grains could be syn- to post-tectonic Carboniferous granites, mesothermal gold deposits and granite-pegmatite-hosted W–Sn mineralization owing to high elevated Sn and W concentrations in detrital rutile grains.

Keywords: detrital rutile, U–Pb, trace elements, Jurassic sandstone, Sakarya Zone, NW Türkiye

Introduction

Trace element geochemistry of detrital grains (e.g., zircon, rutile, garnet, titanite) within clastic sedimentary rocks has provided a rich source of knowledge on the rock units where they are incorporated in such as exceedingly relevant information about revealing petrological and tectonic processes (Okay et al. 2011; Şengün et al. 2020a; Pereira et al. 2021; Schönig et al. 2022; Rösel et al. 2025; Yaşar et al. 2025), trace mineral deposits (Shi et al. 2012; Che et al. 2013; Pereira & Storey 2023), crustal recycling (Andersen et al. 2022). Rutile, one of these detrital grains, contains significant amounts of trace elements and is widely ubiquitous in many magmatic, metamorphic and especially clastic sedimentary rocks, as well as in some hydrothermal systems because it withstands weathering and transport extremely well (Force 1980; Morton & Hallsworth 1994; Meinhold 2010). Clastic sedimentary rocks are widely distributed in a wide variety of depositional environments, which underlines their usefulness in various basic and applied research areas (Galloway & Hobday 1983; Pettijohn et al. 1987; Jamil et al. 2021). Detrital rutile grains are often used as a provenance indicator for clastic sedimentary rocks based on the Nb and Cr concentrations (Triebold et al. 2012; Avigad et al. 2017; Rösel et al. 2019; Pereira et al. 2020; Şengün et al. 2020a; Ershova et al. 2024). Nb/Cr ratios of detrital rutile grains are known to discriminate the pelitic source rocks from the mafic source rocks (e.g., Zack et al. 2004; Meinhold et al. 2011; Rösel et al. 2019; Ershova et al. 2024).

Rutile is well suited to estimate temperature conditions in the source of clastic rocks using the Zr-in-rutile thermometer

✉ corresponding author: Fırat Şengün
firatsengun@comu.edu.tr

(Zack et al. 2004; Tomkins et al. 2007; Kohn 2020). Rutile grains develop in metamafic and metapelitic rocks various ranges of pressure–temperature conditions. Thus, detrital rutile grains have an advantageous when tracking sediment input from the greenschist to amphibolite or granulite-facies sources (e.g., Meinhold 2010; Zack & Kooijman 2017).

Rutile is also one of the minerals used for U–Pb age determination in provenance studies, which records the age of the latest medium to high-grade metamorphic event of source rocks (e.g., Okay et al. 2011; Avigad et al. 2017; Rösel et al. 2019; Şengün et al. 2020a; Ershova et al. 2024; Yaşar et al. 2025). This is because detrital rutile has a low closure temperature for Pb rutile (500–600 °C) (Vry & Baker 2006; Kooijman et al. 2010). Therefore U–Pb dating of such rutile grains provides the timing of the lead closure temperature in rutile during upper amphibolite to lower granulite-facies metamorphism. The rutile U–Pb age data were used to derive the age of metamorphic events within the source area in this study.

This study presents combined trace element geochemical data and U–Pb age determinations of detrital rutile from the Jurassic Bayırköy Formation of the western Sakarya Zone and its metamorphic conditions. The combination of chemical composition with U–Pb dating of rutile and provenance discrimination relationships, including mineralogical fingerprints such as the Cr–Nb provenance discrimination, leads to a more robust toolkit for provenance determination. The aim of this paper is to provide information on the timing of metamorphic event of the source rocks and to reveal the geochemical composition of the source rocks and metamorphic conditions based on detrital rutile grains within the Jurassic Bayırköy Formation. The origin of the clastic rocks in the Jurassic Bayırköy Formation and their genetic relationship with the Variscan orogeny play a fundamental role in the Mesozoic paleotectonic reconstruction of Türkiye.

Geological setting

Türkiye is commonly subdivided into several tectonic zones separated by ophiolitic suture zones representing the closure of branches of Tethyan ocean basins during the Mesozoic and Cenozoic (e.g., Şengör & Yılmaz 1981; Okay & Tüysüz 1999; Moix et al. 2008, Fig. 1). Northwestern Anatolia is known as region where different tectonic units meet, forming one of the critical regions in the geology of Türkiye (e.g., Okay & Satır 2000a; Şengün et al. 2011; Aysal et al. 2012; Okay & Topuz 2017; Karslı et al. 2020; Topuz et al. 2020). The Sakarya Zone, one of these crustal units, is E–W-trending continental sliver bordered by the İstanbul Zone, Thrace Basin in the north, by the Anatolide–Tauride Block and Tavşanlı Zone in the south (Fig. 2a). The complex pre-Jurassic basement of the Sakarya Zone contain three distinct tectonic rock units: (i) Carboniferous amphibolite–granulite-facies metamorphic basement rocks of the Kazdağ, Uludağ, Kurtoğlu, and Pulur Massifs dated by U–Pb using monazite and zircon minerals with an age ranging from 310 to 334 Ma (Topuz & Altherr 2004; Okay et al. 2006; Topuz et al. 2007; Erdoğan et al. 2013, Fig. 1). (ii) Silurian, Devonian, Carboniferous and Permian granitoids cutting these metamorphic basement rocks (Okay et al. 1996; Topuz et al. 2004; Aysal et al. 2012a, b; Sunal 2012; Şengün & Koralay 2017; Karslı et al. 2020; Şengün et al. 2020b; Topuz et al. 2020). (iii) Permo–Triassic Karakaya Complex composed of lower Karakaya Complex and upper Karakaya Complex (Okay & Göncüoğlu 2004).

Conglomerate, sandstone, mudstone and claystone intercalations of the Early Jurassic Bayırköy Formation unconformably overlie the pre-Jurassic basement of the Sakarya Zone (Fig. 2b). The Jurassic Bayırköy Formation exposes in the Gönen region located on the western part of the Sakarya Zone (Fig. 2b). The Bayırköy Formation mainly consists of sandstone with alternations of conglomerate, mudstone and marl in the Gönen region with a thickness of up to 600 m and unconformably rest over the Karakaya Complex with greenschist-facies metamorphic rocks (Fig. 3). The sandstones of the Jurassic Bayırköy Formation are chiefly classified as arkose, subarkose and litharenite based on the major element geochemistry and modal abundances of their framework components (Şengün & Koralay 2019). The Bayırköy Formation commence with coarse-grained conglomerate at the bottom and passes up to medium to coarse-grained sandstone. Fine-grained marl occurs on top of the Bayırköy Formation. This uppermost level of the Bayırköy Formation is separated as nodular limy levels, clayey and marly nodular levels. Clast to matrix-supported conglomerates is characterized by reddish yellow-colored, coarse-grained, cross-bedding and well-sorted pebbles consisting of quartzite, limestone, granite and basalt. Based on the fossil fauna reported from red nodular ammonitico rosso limestones intercalated within these clastic rocks, the age of the Bayırköy Formation is given as Hettangian–early Pliensbachian (Okay et al. 1991). The Jurassic Bayırköy Formation in northwestern Türkiye was deposited in a mixed continental–marine setting, reflecting the transition from fluvial–deltaic systems into shallow marine environments. The lower levels are represented by fluvial and deltaic deposits (conglomerate) indicating river-influenced sedimentation. The middle levels exhibit shoreface to tidal flat facies, which suggests a coastal transition zone with tidal influence. The upper levels including shallow marine carbonates and fossiliferous horizons (ammonites, brachiopods, benthic foraminifera) marking a marine transgression into a shelf environment (Altıner et al. 1991).

The Bayırköy Formation is unconformably overlain by Ammonitico Rosso type carbonates of the Bilecik Limestone. Fossil assemblages documented in this unit such as gastropods, ammonites, belemnites, bivalves, crinoids, brachiopods and foraminifera were identified and assigned to Sinemurian–Pliensbachian age (Altınlı 1973; Altıner et al. 1991; Akyürek et al. 1996). Oligo–Miocene volcanic rocks consisting of andesite, basalt unconformably overlie the Mesozoic sedimentary rocks. Pliocene sedimentary rocks unconformably cover all units in the Gönen region (Fig. 3).

Fig. 1. Tectonic map of the Black Sea region showing the distribution of pre-Jurassic basement outcrops and Jurassic Bayırköy Formation in northern Türkiye (modified after Okay & Nikishin 2015). IAES: Izmir–Ankara–Erzincan suture, IPS: Intra-Pontide suture, ITS: Inner Tauride suture. Isotopic ages are from Okay & Topuz (2017) and Şengün et al. (2020b).

Samples and analytical techniques

Two sandstone samples (sample 2428, 35S 0546666N–35S 4445380E; sample 2432, 35S 0545785N–35S 4446484E) from the Jurassic Bayırköy Formation were selected for trace element and U–Pb isotope analyses of rutiles. The sample locations are given in Fig. 2b.

Heavy mineral separation has been fulfilled on the two sandstone samples (2428, 2432) using traditional techniques of crushing, sieving, magnetic separation and heavy liquids. Clean and inclusion-free detrital rutile grains were separated under a binocular microscope. Hand-picked detrital rutile grains were embedded in epoxy resin and polished down to 1 μm for LA-ICP-MS analyses.

Sample 2428 was taken from light brown-colored, medium to coarse grained, well-bedded sandstone that is representing the lower part of the Bayırköy Formation (Figs. 3 and 4a). Between 10–20 cm thick sandstone layers, 3–6 cm thick mudstone layers occur (Fig. 4b). The sandstone sample mainly has the mineral assemblages of quartz (~54 %), K-Feldspar (~7 %) and rock fragments (~29 %), which are cemented by carbonate (~10 %) (Fig. 4c). Zircon, rutile and apatite minerals have been detected as heavy mineral phases in the sandstone. Quartz is a dominant framework grain in this sandstone sample and occurs as both monocrystalline grains (Qm) and polycrystalline grains (Qp). Subangular monocrystalline quartz is the most abundant component and indicates straight to slightly undulose extinction. The polycrystalline quartz grains have elongated shape, undulose extinction and irregular to crenulated intercrystalline boundaries, which suggests originated from metamorphic source rocks (Fig. 4d). K-feldspar has large crystals, grayish white to yellowish colors and is readily identified by Carlsbad twinning, whereas plagioclase is characterized by gray color and polysynthetic twinning. Rock fragments constituting 29 % of sandstone sample are chiefly composed of a mix of volcanic (Lv) and metamorphic (Lm) rock fragments (Fig. 4e).

Sample 2432 was collected from the upper part of the Bayırköy Formation. The mineralogical components of sample 2432 is mainly made up of quartz (~49 %), K-feldspar (~10 %) and rock fragments (~28 %). The sandstone sample 2432 is cemented by silica and carbonate with amounts varying from 4 % to 9 %. Plagioclase and K-feldspar grains usually are subrounded to subangular-shaped and constitute 10 % of the sandstone sample, which is widely replaced by sericite. Volcanic rock fragments consist of fine-grained basaltic/andesitic rock fragments. However, metamorphic rock fragments are usually composed of polycrystalline quartz grains that are derived from high grade metamorphic sources (Fig. 4f).

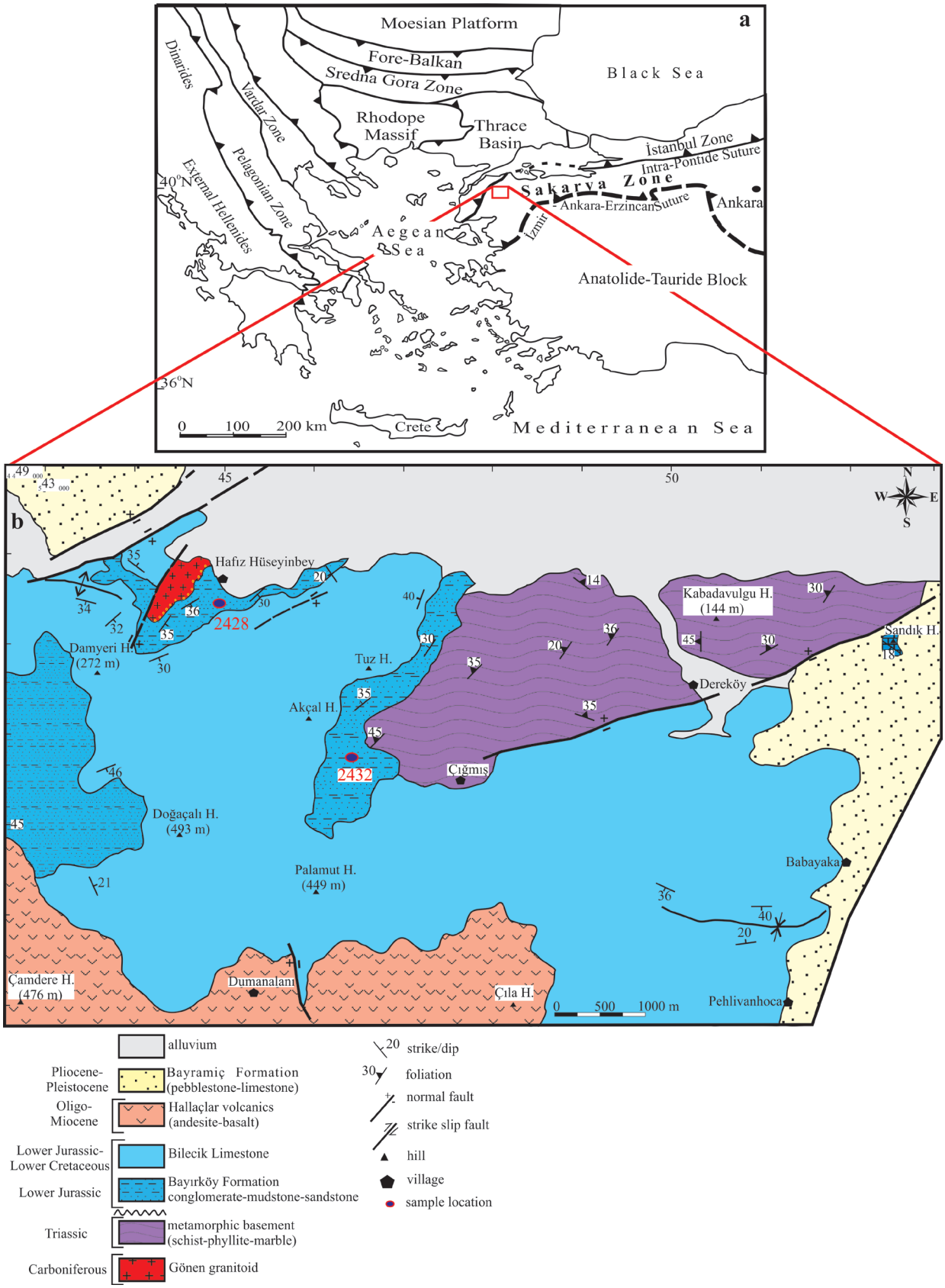

Fig. 2. (a) Simplified geotectonic map of the Eastern Mediterranean region (after Okay & Tüysüz 1999; Meinhold et al. 2011); **(b)** Detailed geological map of the Gönen region in the northwestern Sakarya Zone together with the location of the analysed samples (modified from Yiğitbaş et al. 2010).

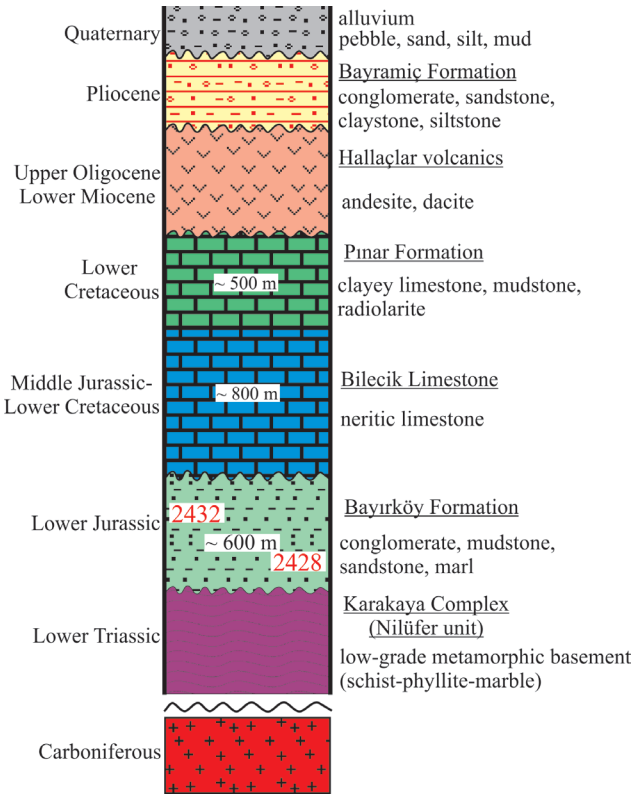

Fig. 3. Generalized stratigraphic section of Mesozoic sedimentary sequences in the northwestern Sakarya Zone and the unconformably overlying Oligo–Miocene and Pliocene covers.

LA-ICP-MS analyses

Laser ablation inductively coupled plasma mass spectrometry (LA-ICP-MS) was used to determine trace element concentrations as well as U–Pb ages of the rutile grains. Clear, crack and inclusion-free detrital rutile grains from both sandstone samples were selected. The trace element and U–Pb analyses were performed simultaneously by LA-ICP-MS at the Institute for Geoscience, Johannes Gutenberg University in Mainz using an ArF Excimer Laser (NWR 193, ESI New Wave) equipped with a TwoVol2 ablation cell, coupled to an Agilent 7700x ICP-MS instrument. Detailed information regarding equipment and instrumental conditions used for analyses is listed in Supplementary Table S1. Analyses were performed using a laser beam diameter of 30 µm with a beam energy density of ~3.5 J cm^{-2} and a repetition rate of 10 Hz. Each analysis consisted of 15 s of background measurement during laser warm-up, 30 s of ablation and 20 s of washout. Monitored isotopes included ^{27}Al, ^{45}Sc, ^{49}Ti, ^{51}V, ^{52}Cr, ^{56}Fe, ^{59}Co, ^{60}Ni, ^{66}Zn, ^{89}Y, ^{90}Zr, ^{93}Nb, ^{95}Mo, ^{118}Sn, ^{121}Sb, ^{178}Hf, ^{181}Ta, ^{182}W, ^{206}Pb, ^{207}Pb, ^{208}Pb, ^{232}Th, and ^{238}U. At the beginning and after every 10 spots on the samples, NIST SRM 610 (Jochum et al. 2011), rutile R10 (Luvizotto & Zack 2009), as well as basaltic USGS BCR-2G (Jochum et al. 2005) were analyzed.

Trace element analysis of detrital rutiles

For the trace element determinations Ti measured as ^{49}Ti was used as the internal standard element applying a mass fraction of 98.4 wt% TiO_2 (59 wt% Ti) for rutile grains. The synthetic glass NIST SRM 610 was used for calibration applying the preferred values available from the GeoReM database (http://georem.mpch-mainz.gwdg.de/; compare also Jochum et al. 2005, 2011). Basaltic USGS BCR-2G and rutile R10 (Luvizotto & Zack 2009) were used to monitor accuracy and reproducibility of the analysis and calibration strategy. The time-resolved signal was processed using the program Iolite 4 (Paton et al. 2011) using Trace Elements data reduction scheme (DRS) (Supplementary Table S2). Results for the quality control material agree well with the range of published values reported in the GeoReM database (http://georem.mpch-mainz.gwdg.de/). Trace element mass fractions of reference materials and detrital rutile grains are given in Supplementary Tables S4 and S5.

Zr-in-rutile thermometer

Zr-in-rutile thermometer is based on the zirconium content in rutile coexisting with quartz and zircon. The Zr contents of detrital rutile grains provide crucial information about the temperature of the latest metamorphic event based on the equilibrium with zircon and quartz in the host rock (Zack et al. 2004). The Tomkins et al. (2007) thermometer was used for the calculation of Zr-in-rutile temperatures for each rutile grain, which considering as pressure of 10 kbar. The calibration of Tomkins et al. (2007) with a pressure correction is a trustworthy thermometry for medium to high-grade metamorphic rocks, which gives more reliable temperatures than any other exchange thermometers (e.g., Miller et al. 2007; Luvizotto & Zack 2009).

U–Pb dating of detrital rutile grains

Signal intensities of the isotopes (^{206}Pb, ^{207}Pb, ^{208}Pb, ^{232}Th, and ^{238}U) were reduced in Iolite 4 (Paton et al. 2011) using VizualAgeUcomPbine DRS (Chew et al. 2014, Supplementary Table S3). Common Pb correction in the reference material and detrital rutile grains was based on the model Pb composition of Stacey & Kramers (1975) (Supplementary Table S6). The IsoplotR (Vermeesch 2018) was used to calculate ^{207}Pb/^{235}U and ^{206}Pb/^{238}U ages from the respective ratio from the Iolite output data table (Supplementary Table S7). The Tera-Wasserburg lower intercept ages were used for interpretation and discussion. All age uncertainties are given as 2s level in the text.

Results

Detrital rutile grains are yellowish to reddish brown colour and have mostly well-rounded shapes showing detrital origin

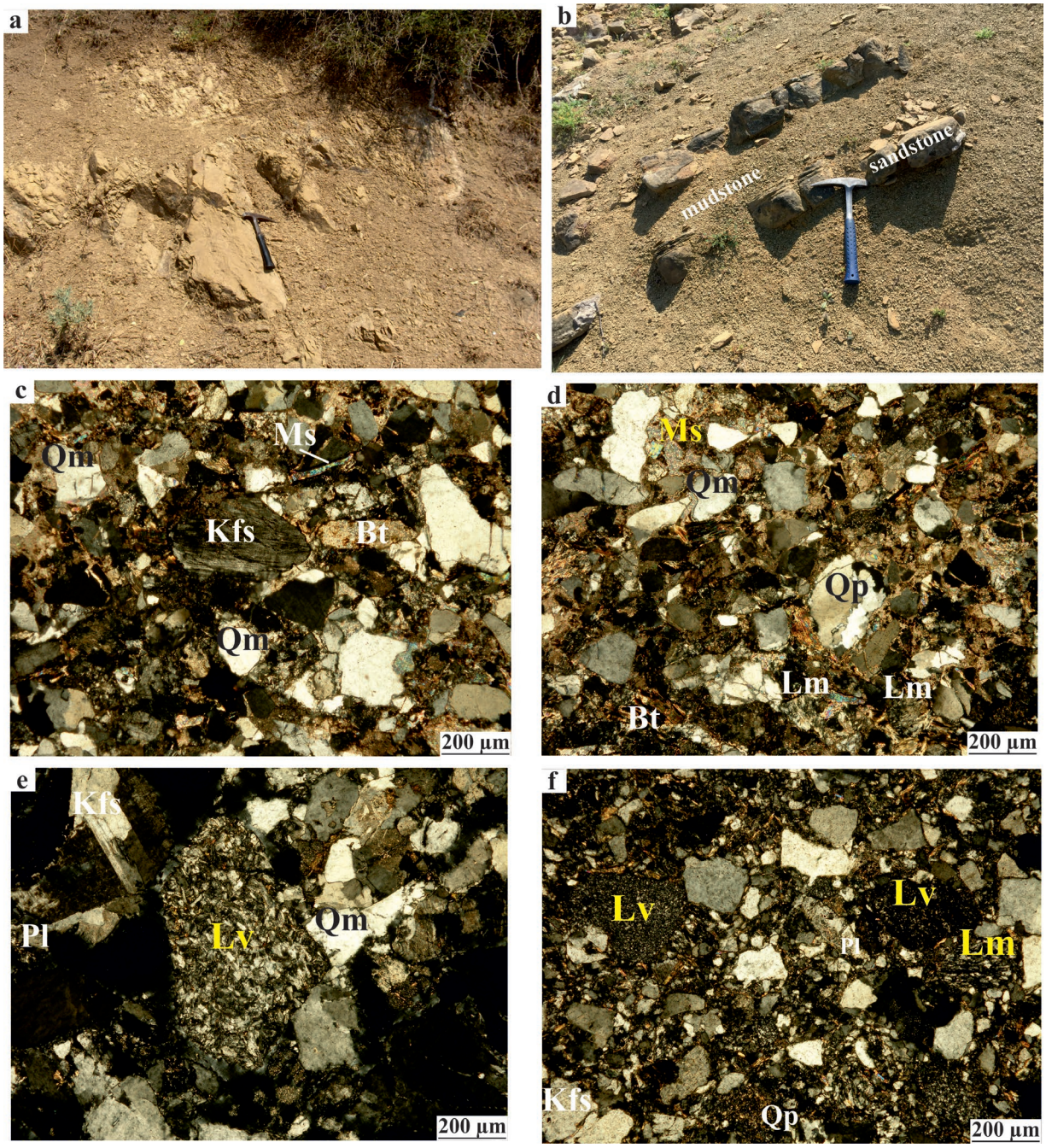

Fig. 4. (a) Field view of brown-coloured, medium to coarse-grained sandstone (35S 0545780N–35S 4446458E); **(b)** thin-bedded sandstone and thin-bedded siltstone alternation in the Jurassic Bayırköy Formation (35S 0545484N–4447377E); **(c)** Photomicrograph of analysed Jurassic sandstone including subrounded monocrystalline quartz grains with straight extinction; **(d)** Polycrystalline quartz grain showing subgrains with straight to slightly curved intercrystalline boundaries; **(e)** Volcanic rock fragments with basaltic/andesitic origin; **(f)** Metamorphic fragments represented by elongated quartz grains (all the photomicrographs are observed in cross-polarized light, Qm: monocrystalline quartz, Qp: polycrystalline quartz, Kfs: potassium feldspar, Pl: plagioclase, Bt: biotite, Ms: muscovite, Lv: volcanic fragment, Lm: metamorphic fragment, mineral abbreviations after Kretz 1983).

in the two sandstones samples. From each of the two samples, 110 detrital rutile grains were separated. Thus, trace element composition of 220 rutile grains in the studied sandstone samples from the Jurassic Bayırköy Formation were determined by LA-ICP-MS and the results are given in Supplementary Table S5. All detrital rutile grains were further analysed for their U and Pb isotopic composition (Supplementary Table S7). For some grains, the signals for the different Pb and U isotopes were unstable. Such analyses were not further processed for U–Pb ages and are indicated respectively in the tables.

Trace element composition of detrital rutile grains

Sample 2428

Detrital rutile grains are mostly elongated, 150–250 µm long and show quartz inclusions and tiny ilmenite lamellae (Fig. 5a). Nb concentrations in detrital rutile have a wide range varying between 80 µg/g and 11600 µg/g. However, Cr contents vary from 20 µg/g to 5700 µg/g. Most detrital rutile grains are classified as metapelitic according to the source rock discrimination diagram of Triebold et al. (2012) in Fig. 6a (82 % metapelitic source, 18 % metamafic source). The Zr contents in detrital rutile grains range between 20 µg/g and 1400 µg/g. The Zr-in-rutile temperature estimations for the detrital rutile grains for 10 kbar α-Quartz after Tomkins et al. (2007) and are illustrated in Fig. 6b. The temperatures calculated for rutile grains in sample 2428 range from 480 °C to 790 °C with an average of 665 °C (Fig. 6b). Detrital rutile grains mostly yield Zr-in-rutile temperatures that agree with amphibolite-facies metamorphic conditions, which range between 500 and 750 °C. Only a minority of detrital rutile grains indicate Zr-in-rutile temperatures equivalent to greenschist-facies (450–500 °C) and granulite-facies metamorphic conditions (750–800 °C).

Hf and Ta concentrations exhibit large variations (Hf: 0.1–125 µg/g, Ta: 2.7–1564 µg/g). Nb/Ta ratios of 110 metapelitic and metamafic detrital rutile grains vary from 4 to 64 with a mean value of 18. Most of the detrital rutile grains agree largely with subchondritic Nb/Ta ratios (Fig. 7a; chondritic Nb/Ta=19.9 value from Münker et al. 2003). However, 15 of detrital rutile grains have suprachondritic Nb/Ta ratios (20–38 with an average of 28) (Fig. 7a,b). On the other hand, all the metapelitic and metamafic detrital rutile grains, except for thirteen, have subchondritic Zr/Hf ratios (4–59) compared to the chondritic Zr/Hf value of 34.3 (Fig. 7b; Münker et al. 2003).

Sample 2432

Detrital rutile grains are mostly rounded in shape, indicating a sedimentary origin (Fig. 5b). Some rutile grains are elongated in shape and contain ilmenite, zircon, and quartz inclusions. Most of the grains are dark brown and have homogenous chemical composition. The Nb and Cr contents in rutile grains are in the range of 40–11900 µg/g and 6–4600 µg/g, respectively. Most of the detrital rutile grains were plotted for source discrimination on the Cr–Nb diagram (Fig. 6a). 58 % of the detrital rutile grains were sourced from metapelitic and 42 % from metamafic rocks based on the Cr–Nb ratios. Zr concentrations in both metapelitic and metamafic detrital rutile grains vary between 40 µg/g and 1400 µg/g. Zr-in-rutile temperatures calculated by the calibration of Tomkins et al. (2007) range from 510 °C to 790 °C with an average temperature of 605 °C at 10 kbar (Fig. 6c). Temperatures estimates exhibit that metapelitic and metamafic rutile grains grew under amphibolite-facies metamorphic conditions, whereas a few detrital rutile grains have Zr-in-rutile temperatures showing granulite-facies metamorphic conditions.

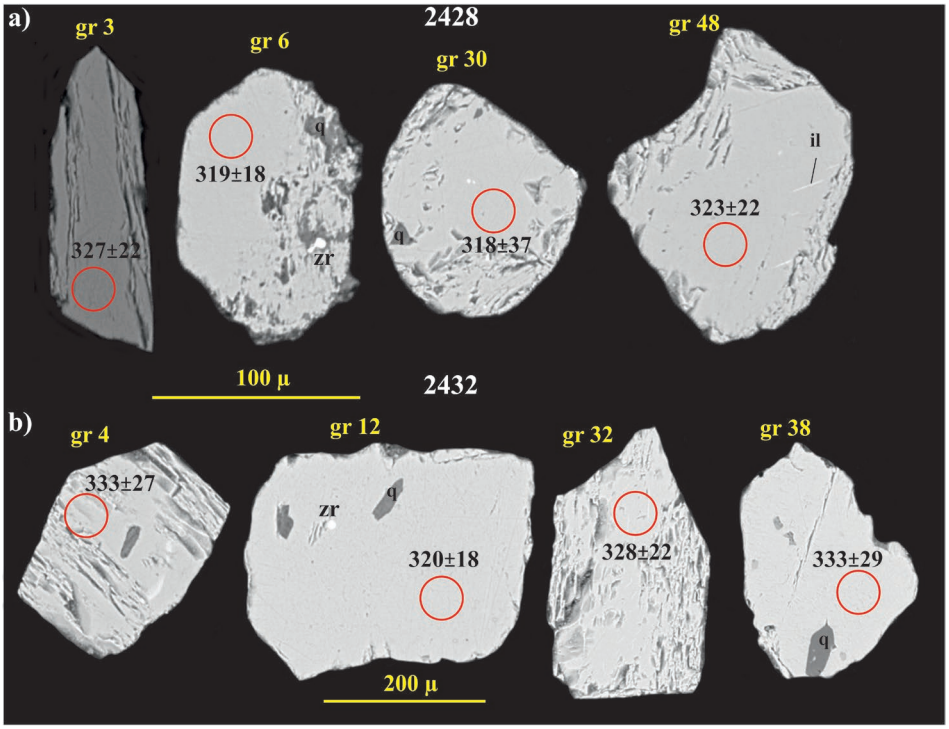

Fig. 5. BSE images of some rutile grains from sample 2428 **(a)** and sample 2432 **(b)**. Red circle refers to the laser spots (30 µm) for U–Pb and trace element analyses (q: quartz, il: ilmenite, zr: zircon).

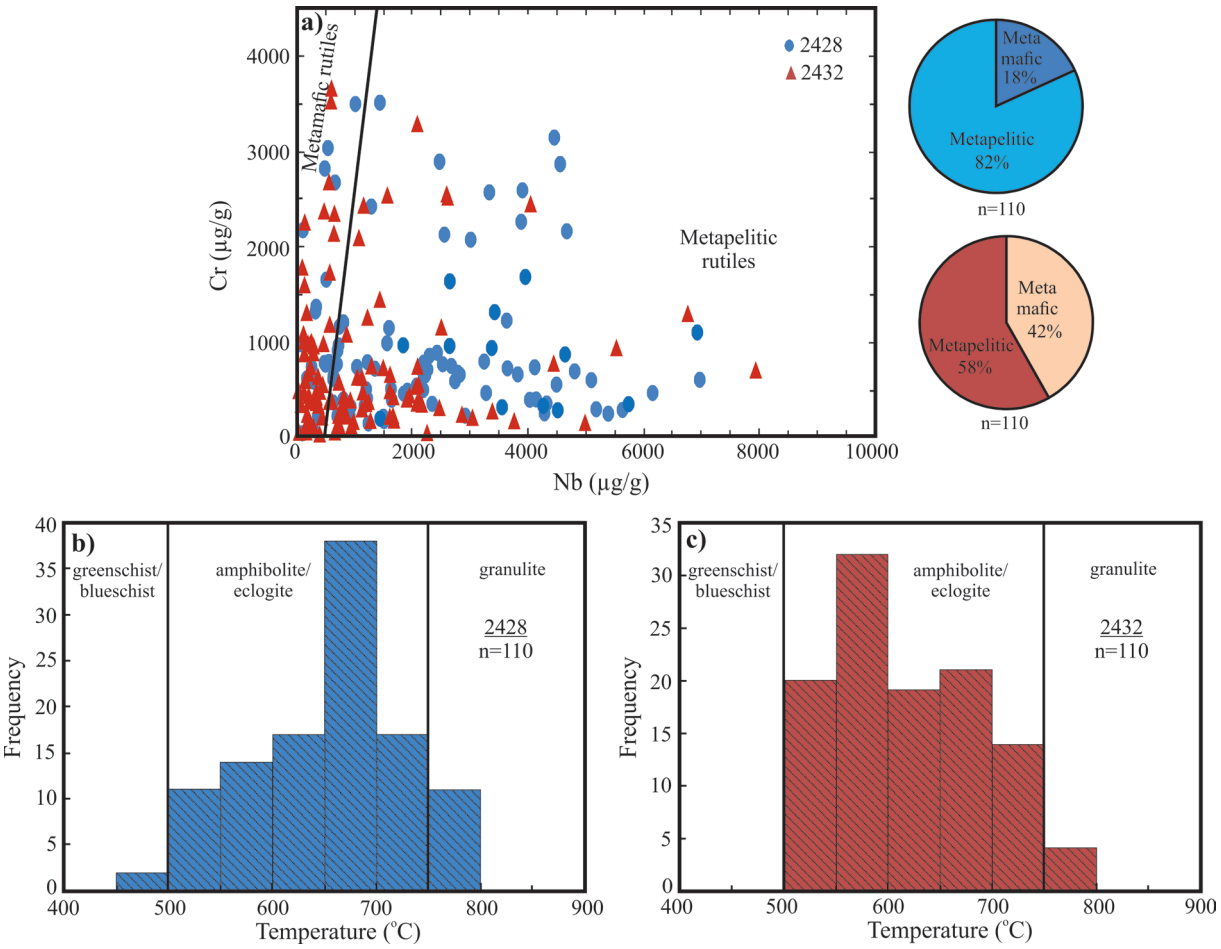

Fig. 6. (a) Cr–Nb source rock discrimination from the detrital rutile grains analysed in this study. The classification into metapelitic and metamafic follows Triebold et al. (2012). **(b, c)** Zr-in-rutile temperature distributions. Zr-in-rutile temperatures were calculated according to Tomkins et al. (2007) assuming a pressure of 10 kbar in the α-quartz field. Temperatures below approximately 500 °C correspond to greenschist/blueschist facies, between approximately 500 °C and approximately 750 °C to amphibolite and eclogite facies and above 750 °C to granulite facies.

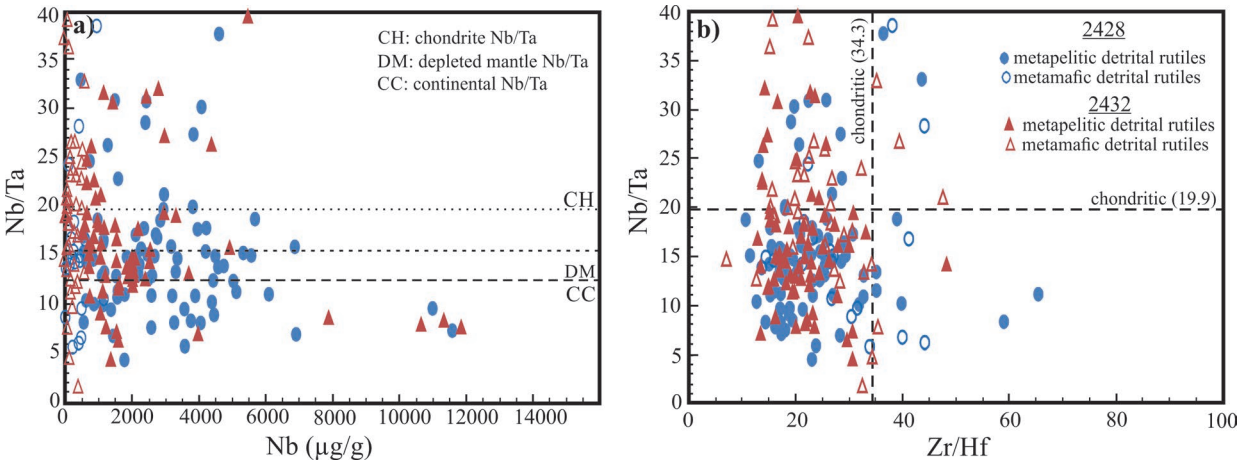

Fig. 7. Element ratio plots. Points represent individual analyses. **(a)** Nb versus Nb/Ta. **(b)** Zr/Hf versus Nb/Ta diagram. Nb/Ta and Zr/Hf of rutile are usually subchondritic. Dashed lines refer to chondritic values for continental crust, depleted mantle, Nb/Ta and Zr/Hf (Barth et al. 2000; Münker et al. 2003).

Metapelitic and metamafic detrital rutile grains have Ta and Hf concentrations of 0.45–1526 μg/g and 0.32–110 μg/g, respectively. The 110 detrital rutile grains have Nb/Ta ratios varying from 2 to 49 with a mean value of 20. While most of the detrital rutile grains have subchondritic Nb/Ta ratios (chondritic Nb/Ta=19.9 value from Münker et al. 2003), there are 16 detrital rutile grains from this sandstone that have superchondritic Nb/Ta values (Fig. 7a). In contrast, all metapelitic and metamafic detrital rutile grains have subchondritic Zr/Hf (7–48) ratios compared to the chondritic Zr/Hf value of 34.3 (Fig. 7b; Münker et al. 2003) whereas four grains yield suprachondritic Zr/Hf ratios. Nb/Ta, Nb concentrations, and Zr/Hf ratios (Fig. 7a, b) overlap with each other in both metapelitic and metamafic detrital rutile grains, which reflects the compositions of the source rocks.

U–Pb geochronology of detrital rutile grains

Tera-Wasserburg plots for all samples with 2σ error ellipses (Fig. 8a, c) and the respective Kernel density estimation (KDE) plots for single analyses concordia ages (Fig. 8b, d) were illustrated using IsoplotR (Vermeesch 2018). Analyses that have uncertainties (2σ) for the $^{206}Pb/^{238}U$ age and $^{207}Pb/^{235}U$ age below the cut-off threshold calculated following Chew et al. (2020) are the most precise for both U decay systems. Seventy-two detrital rutile grains from sample 2428 and fifty-three detrital rutile grains from sample 2432 were measured for their U–Pb isotope composition. U concentrations of dated samples range between 2 μg/g and 232 μg/g. This age data is more representative for the whole detrital rutile ages as rutile grains with low U and/or higher amounts of common ^{208}Pb are excluded.

19 detrital rutile grains out of 91 rutile grains from sample 2428 were not included in the calculations due to low U content. The $^{238}U/^{206}Pb$ ages range between 244 Ma and 606 Ma. The lower intercept $^{238}U/^{206}Pb$ age of detrital rutile grains is 313±10 Ma (n=72, MSWD=2.6; Fig. 8a). However, six detrital rutile grains have Ediacaran ages varying between 555 Ma and 606 Ma (Fig. 8b).

53 detrital rutile grains from sample 2432 out of 90 detrital rutile grains yield single-analyses concordia ages (Fig. 8c). The $^{238}U/^{206}Pb$ ages from 53 detrital rutile grains have varying from 212 Ma and 694 Ma. The lower intercept $^{238}U/^{206}Pb$ age of detrital rutile grains is 330±12 Ma (n=53, MSWD=2.5; Fig. 8c). On the other hand, eleven rutile grains and four rutile grains yield Ediacaran ages ranging from 541 Ma to 694 Ma, and Triassic ages between 212 Ma and 251 Ma, respectively (Fig. 8d).

Discussion

Detrital rutile provenance of the Jurassic sandstones

The trace element composition and Zr-in-rutile thermometry of detrital rutiles from the Jurassic sandstones give significant information about their source rocks. The Cr vs Nb diagram allowed to discriminate between felsic and mafic sources. The enrichments in Nb or Cr also reflect the mafic from more felsic sources through fluid path or in its source even though this discrimination diagram was initially designed to separate felsic from mafic metamorphic source rocks (Zack et al. 2004). Based on the Cr and Nb concentrations, the detrital rutile grains have been classified as metapelitic and metamafic lithologies in origin (Fig. 6a). 70 % of the analysed detrital rutile grains from the two sandstone samples were derived from metapelitic rocks, whereas 30 % of the rutile grains yield the typical composition for those originated from metamafic rocks.

The rutile formation temperatures from detrital rutile grains were calculated by the Tomkins et al. (2007) calibration. The Paleozoic continental basement of the Sakarya Zone is represented by metamorphic rocks chiefly composed of orthogneiss, paragneiss, quartzofeldspathic schist intercalated with amphibolite, eclogite and marble lenses and granitic rocks (Okay et al. 1996). The main mineral assemblage of these felsic metamorphic rocks dominantly consists of quartz, plagioclase, garnet, biotite, muscovite and rare sillimanite, which gives the P–T metamorphic conditions of 5–11 kbar and higher than 600 °C (Okay & Satır 2000a; Topuz et al. 2007, 2020; Aygül et al. 2012). However, the P–T conditions of the metamafic rocks (amphibolite, metagabbro, eclogite) were estimated as 9–24 kbar at 450–650 °C according to the mineral assemblage of amphibole, garnet, phengite, omphacite, epidote (Okay & Satır 2000a, b; Okay et al. 2002, 2006; Şengün & Zack 2016). These P–T conditions indicate that the metamorphic basement in the western Sakarya Zone underwent the amphibolite-facies metamorphism. Zr concentrations of most metapelitic detrital rutile grains from two sandstone samples vary from 30 μg/g to 1400 μg/g, which yields Zr-in-rutile temperatures between 500 °C and 790 °C. However, all metamafic detrital rutile grains have Zr concentrations ranging from 20 μg/g to 1300 μg/g, which correspond to 480–780 °C at 10 kbar. Metapelitic and metamafic source rocks have distinct Zr-in-rutile temperatures due to difference in fluid composition. Thus, detrital rutile grains in the metamafic rocks could have grown from different fluid at lower temperatures than those of the metapelitic rocks. The Zr-in-rutile temperatures and Cr–Nb discrimination diagram pointed that the potential source area for sandstones in the Jurassic Bayırköy Formation was dominated by the amphibolite-facies metamorphic rocks (Fig. 6b, c). Detrital rutiles grains from the metapelitic rocks sourced from paragneiss, mica schist, whereas metamafic detrital rutiles possibly originated from amphibolite, eclogite and metagabbro. On the other hand, less detrital rutile grains underwent the conditions of granulite-facies metamorphism.

Nb/Ta ratios of rutile can be used as a tracer of geochemical processes during subduction zone metamorphism, crustal–mantle differentiation through magma evolution and element cycling (e.g., Foley et al. 2000; Ding et al. 2009). Detrital rutile grains from two sandstone samples have a wide range of

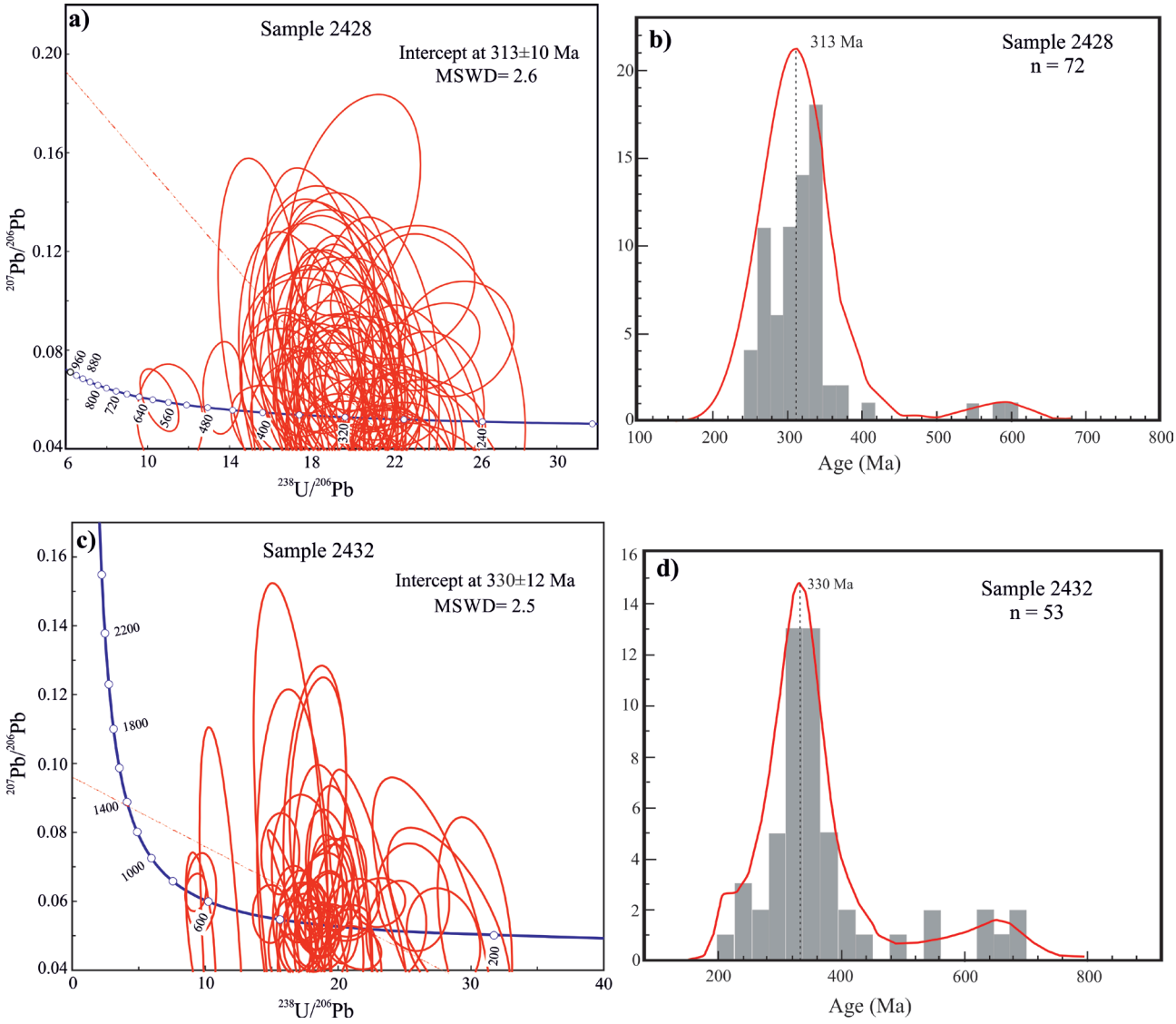

Fig. 8. (a, c) Tera-Wasserburg concordia diagrams for detrital rutile ages (sample 2428 and sample 2432). Rutile ages are plotted with 2σ error ellipses. **(b, d)** Detrital rutile U–Pb age data distributions (KDE). The bandwidth of the histograms and the bandwidth for the KDE plots are 20 and 40, respectively. Single-analyses concordia ages are used for the KDE plots and common ^{208}Pb corrected ratios for the Tera-Wasserburg concordia diagrams. n=number of dated rutile grains.

Nb/Ta ratios and relatively similar Zr/Hf ratios compared to metamorphic rutile (Fig. 7). The metapelitic detrital rutile grains give the Nb/Ta ratios ranging between 4 and 64, whereas the Nb/Ta ratios of metamafic detrital rutile grains vary from 2 to 58. The metapelitic detrital rutile grains have slightly higher Nb/Ta ratios than those of metamafic detrital rutile grains. The wide range in Nb/Ta for metapelitic detrital rutile grains may have been resulted from the fluid-rock interaction processes. As metapelitic rocks include more water relative to metamafic rocks during metamorphic reactions and hence could have given rise to highly variable values for their Nb/Ta ratios (Liu et al. 2014). Metapelitic and metamafic detrital rutile grains from two sandstone samples frequently have subchondritic Nb/Ta (4–64) and Zr/Hf (4–59) ratios (Fig. 7b). All known mantle and crustal reservoirs have essentially subchondritic Zr/Hf and Nb/Ta ratios (e.g., Foley et al. 2000; Rudnick et al. 2000; Klemme et al. 2005; Meinhold 2010). Comparable Nb/Ta ratios were documented in metapelitic and metamafic rocks from the Devonian–Carboniferous amphibolite-facies clastic rocks in the Istanbul Zone and Central Sakarya Zone (Okay et al. 2011; Şengün et al. 2020a).

Nb/Ta and Zr/Hf ratios also give information about rutile origin such as metamorphic, magmatic and hydrothermal (Pereira et al. 2019). Some detrital rutile grains with very low Nb/Ta ratios indicate that these rutile grains formed in hydrothermal systems (Fig. 9a). Authigenic rutile and rutile from the low-T fluids give low Nb/Ta ratios, since Ta grows more compatible with rutile in the presence of aqueous fluids, combined with low Zr/Hf ratios (Pereira et al. 2019). Most detrital rutile grains have Nb/Ta and Zr/Hf ratios largely occurring in

metamorphic settings, which exhibits that the detrital rutile grains are of a metamorphic origin (Fig. 9b). So, geochemical distribution of detrital rutile grains (Fig. 9) show that these detrital rutile grains were derived from multiple sources. The elevated Fe concentrations (>1000 μg/g) of detrital rutile grains probably give a clue about metamorphic origin, whereas magmatic rutiles generally have less than 1000 μg/g Fe (Zack et al. 2004). The Fe contents of detrital rutile grains from two samples range between 1100 μg/g and 9800 μg/g, which indicates metamorphic origin. However, sixteen rutile grains have magmatic origin with low Fe contents (150–1000 μg/g). Moreover, orogenic gold-related rutile (Sn–W-rich) shows a significant overlap in Nb/Ta ratios that is consistent with metamorphic origin (e.g., Zack et al. 2002; Zeh et al. 2018). Rutile from W–Sn deposits associated with granite pegmatites and gold mineralized rocks contain high Sn and W concentrations (>1000 μg/g) together with high Nb and Ta contents (Rice et al. 1998; Clark & Williams-Jones 2004; Scott 2005). Trace element chemistry indicates that some rutile grains (~21 grains) have higher Sn and W concentrations (>1000 μg/g) as well as Nb and Ta contents, which may have been derived from mesothermal gold deposits and granite–pegmatite-hosted W–Sn mineralization.

Sources of detrital rutile grains in the Jurassic sandstones

The source lithology from all analysed detrital rutile grains is mainly metapelitic (70 %, mica schists, paragneisses). Therefore, metamafic rocks such as eclogites and amphibolites with a great majority of rutile grains were not commonly outcropped at the surface of the source. These eclogitic and amphibolitic rocks are presently exposed in the Bandırma region, where include HP–LT eclogites dates as latest Triassic (208–203 Ma) using Ar–Ar method on phengites (Okay & Monié 1997). The metapelitic and metamafic source lithologies are represented by Variscan high-grade metamorphic overprint (amphibolite-facies metamorphism) at 313–330 Ma (Fig. 8). The 313–330 Ma could be accepted as the age range for the metamorphism of potential source rocks in western Sakarya Zone. However, four rutile grains yield Triassic ages between 212 Ma and 251 Ma, twenty-three rutile grains have the ages between 259 Ma and 291 Ma, and eleven rutile grains Ediacaran ages ranging from 541 Ma to 694 Ma (Fig. 8). All these ages indicate multiple sources for the detrital rutile grains in the Jurassic sandstones. The detrital rutiles with 694–541 Ma populations showing the Gondwana origin. Detrital zircons in paragneisses from the Söğüt region in the Central Sakarya Zone and Eastern Sakarya Zone have also 650–500 Ma populations (Ustaömer et al. 2012, 2013), which consistent with detrital rutile populations from the Jurassic sandstones. Therefore, detrital rutile data demonstrate that Neoproterozoic–Cambrian granites form the pre-metamorphic sequence, which is overlain by the Paleozoic sedimentary and intrusive rocks.

Zr-in-rutile temperatures for the amphibolite-facies metamorphism range between 480 °C and 790 °C. The Variscan high-grade metamorphic basement rocks are present in the Sakarya Zone (Kazdağ, Uludağ, Söğüt, Kurtoğlu and Pulur Massifs), Balkanides (Rhodope Massif, Serbo Macedonian Massif), Pelogonian Zone, Strandja Massif, Lesser (Dzirula Massif) and the Greater Caucasus (Blyp Complex). The metamorphism of these basement rocks in the Sakarya Zone, Strandja Massif, Rhodope Massif, Dzirula Massif can be ascribed to the Variscan orogeny with Carboniferous ages (310–330 Ma) from Kazdağ, Söğüt and Pulur Massifs (Okay et al. 1996, 2001; Carrigan et al. 2006; Topuz et al. 2007; Mayringer et al. 2011; Yaşar et al. 2025).

Amphibolite-facies metamorphic basement rocks of the Kazdağ Massif, Uludağ Massif, Pulur and Kurtoğlu Massif located in the Sakarya Zone are mainly composed of quartz–feldspathic gneiss, amphibole-bearing gneiss, amphibolite, marble, meta-ultramafic rocks with minor migmatite. Zircon ages from the felsic gneisses and amphibolites in the Kazdağ Massif yielded 308–329 Ma, which indicates that the Kazdağ Massif experienced amphibolite-facies metamorphism during the Early Carboniferous (Okay et al. 1996). The Kazdağ

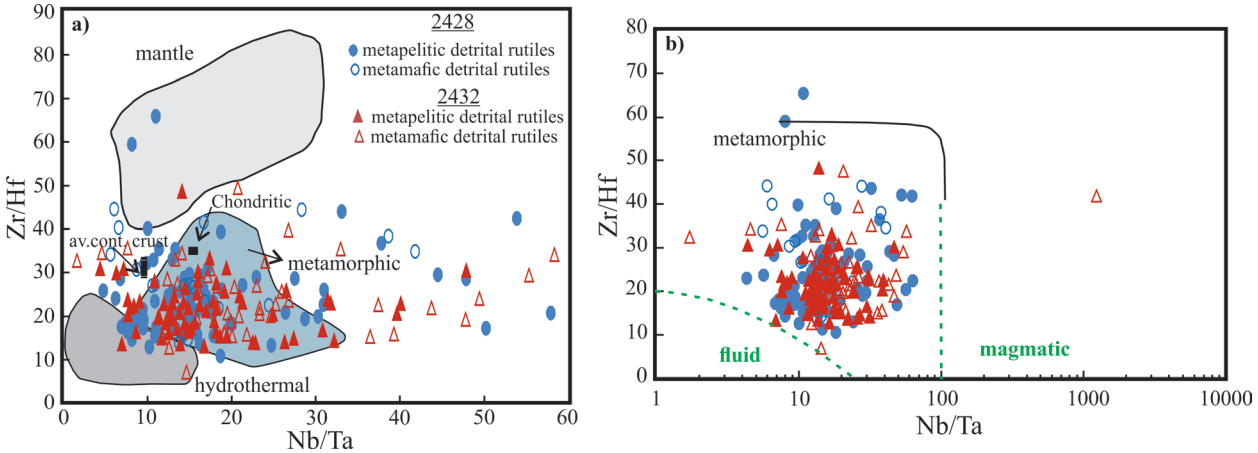

Fig. 9. Zr/Hf vs Nb/Ta discrimination diagrams for detrital rutile with discriminative fields for fluid-related, hydrothermal, metamorphic and magmatic-related rutile (Pereira et al. 2019).

Massif could be compared to the Early Carboniferous amphibolite-facies metamorphic rocks of the Rhodope Massif in Greece, Söğüt, Pulur and Kurtoğlu Massifs in central and eastern Sakarya Zone, and Dzirula Massif in the Lesser Caucasus (Okay et al. 1996; Okay & Satır 2000a; Topuz et al. 2007, 2020; Mayringer et al. 2011; Yaşar et al. 2025). Therefore, the age of amphibolite-facies metamorphic rocks and P–T conditions suggest that these metamorphic basement rocks could be the primary source rocks for the detrital rutiles in the sandstones of the Jurassic Bayırköy Formation from the western Sakarya Zone. On the other hand, detrital rutile grains have magmatic and hydrothermal origin, which shows Carboniferous magmatic source rocks (Fig. 1). These granites mainly expose in the western Sakarya Zone (Gönen granite), in the central Sakarya Zone (Söğüt granite), in the eastern Sakarya Zone (Gümüşhane, Narlık granites), Strandja Massif (Kula, Kırklareli granite), Rhodope Massif (Arda, Byala Reka, Kesebir granites) and in the Lesser Caucasus (Dzirula and Kharami granites), which intrudes amphibolite-facies metamorphic rocks and unconformably overlain by Lower Jurassic continental to marine sedimentary rocks (Fig. 10). U–Pb zircon ages of Carboniferous granites vary from 336 to 294 Ma (Topuz et al. 2010; Gamkrelidze et al. 2011; Mayringer et al. 2011; Okay et al. 2011; Ustaömer et al. 2012, 2013; Machev et al. 2015; Natal'in et al. 2016; Şengün et al. 2020b). They are also derived from mesothermal gold deposits and granite–pegmatite-hosted W-Sn mineralization based on the high Sn–W and Nb–Ta contents. Metapelitic and metamafic detrital rutile grains originated from amphibolite-facies rocks may have been transported into the Early Jurassic basin. The Jurassic sandstones exposed in the western part of the Sakarya Zone were deposited on a passive continental margin of the Jurassic basin. This passive margin was settled on the back-arc side or the southern side of the subduction-related magmatic arc. Sediments derived from the metamorphic basement rocks were transported into the back-arc basin and have geochemical characteristics identical to those of passive continental margin (Şengün & Koralay 2019).

The Early Carboniferous metamorphism from the Sakarya Zone to the Caucasus occurred between 318 Ma and 340 Ma (Fig. 10). Ar–Ar mica, amphibolite and detrital rutile U–Pb ages show that the Söğüt metamorphics underwent the amphibolite-facies metamorphism during the Early Carboniferous (318–346 Ma; Uğurcan et al. 2019; Şengün et al. 2020b; Yaşar et al. 2025). U–Pb monazite age from the Pulur Massif (Topuz et al. 2004) and zircon age from the Narlık region (Ustaömer et al. 2013) in the eastern Sakarya Zone yielded ~330 Ma and 334 Ma, respectively, which reflects the age of regional metamorphism. U–Pb zircon ages constrain the peak metamorphism ranging from 340 to 330 Ma in the Dzirula Massif (Mayringer et al. 2011). U–Pb zircon ages indicate that amphibolite-facies metamorphism took place in the Sredna-Gora

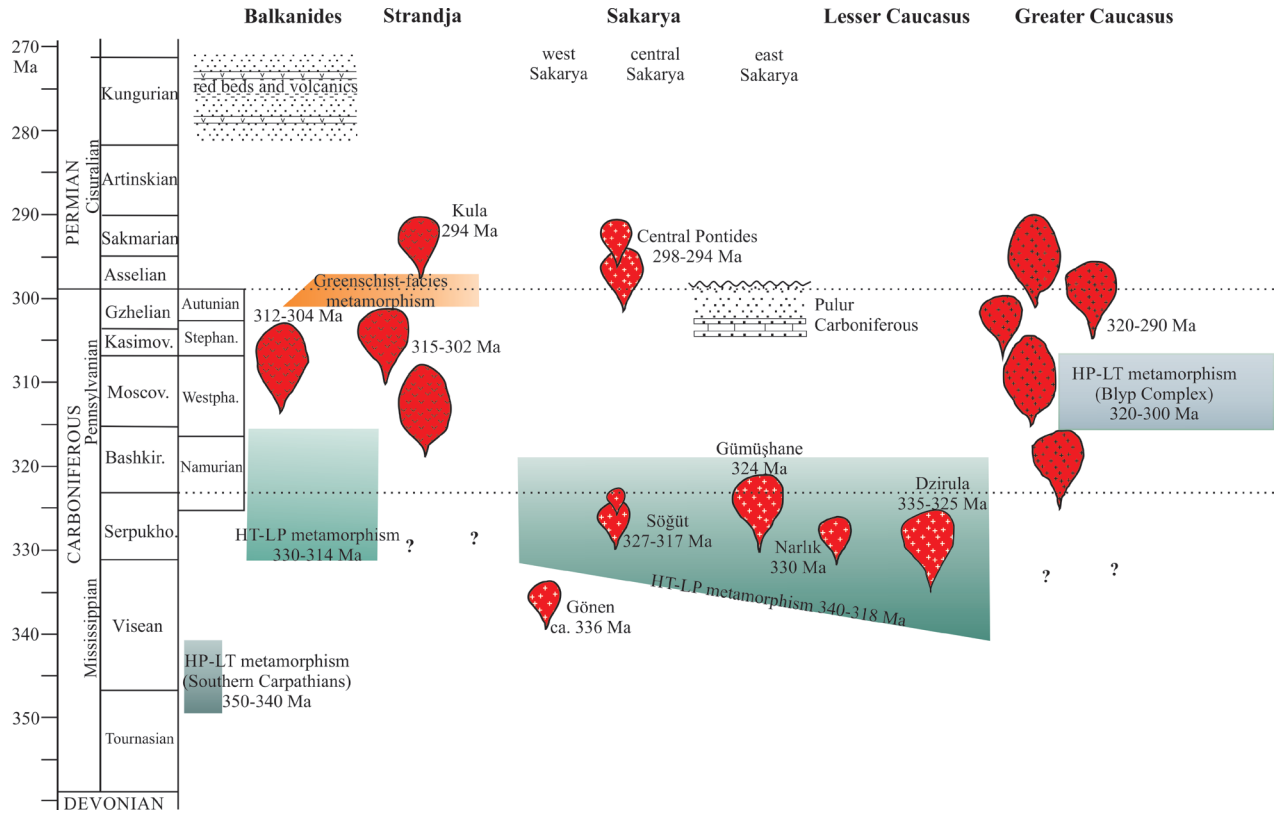

Fig. 10. Magmatic, metamorphic and sedimentary events during the Variscan orogeny in the Sakarya Zone (modified from Okay & Topuz 2017).

Massif in Bulgaria (Balkanides) at ~337 Ma (Carrigan et al. 2006). U–Pb detrital rutile ages from the Carboniferous flysch of the Istanbul Zone yielded Late Devonian–Early Carboniferous metamorphic age and trace element geochemistry exhibits the amphibolite-facies metamorphic source (Okay et al. 2011). Thus, these clastic rocks could be another possible source of detrital rutiles in sandstones from the Jurassic Bayırköy Formation. Moreover, Zr-in-rutile temperatures of metapelitic rutiles were estimated as 550–750 °C that is similar to our detrital rutiles (Okay et al. 2011).

Conclusions

This work provides combined trace element geochemistry and U–Pb dates from detrital rutile grains in sandstones of the Jurassic Bayırköy Formation for their potential source rocks. The following main results are obtained from detrital rutile grains in the western Sakarya Zone.

- According to the Cr–Nb discrimination, the great majority of detrital rutile grains (70 %) are sourced from metapelitic rocks such as mica schist and paragneiss, the rest of detrital rutile grains (30 %) are derived from metamafic rocks such as amphibolite, eclogite and metagabbro. Trace element composition suggests that detrital rutile grains have mostly metamorphic origin and to a lesser extend hydrothermal and magmatic origin.
- Zr contents in most metapelitic detrital rutile grains vary between 30 μg/g to 1400 μg/g, which correspond to the Zr-in-rutile temperatures between 500 °C and 790 °C. However, all the metamafic detrital rutile grains have Zr concentrations ranging from 20 μg/g to 1300 μg/g, which yields 480–780 °C at 10 kbar. The difference in metamorphic temperatures is caused by difference in fluid composition.
- The calculated rutile formation temperatures indicate that the great majority of detrital rutile grains originate from amphibolite-facies metamorphic rocks, whereas less detrital rutile grains were derived from greenschist and granulite-facies metamorphic rocks.
- The lower intercept $^{238}U/^{206}Pb$ ages of detrital rutile grains range from 313±10 Ma to 330±12 Ma, which yields the age of metamorphism for the potential source rocks of detrital rutile grains in the Sakarya Zone.
- Metapelitic and metamafic detrital rutile grains sourced from amphibolite-facies rocks and magmatic rocks in the Jurassic sandstones may have been transported into the sedimentary rocks of the Jurassic Bayırköy Formation before Early Carboniferous time. The Jurassic sandstones exposed in the western part of the Sakarya Zone are consistent with a passive margin setting as stated in the previous studies.
- Trace element geochemistry of detrital rutile grains with their isotopic ages exhibit potentially derivation from metamorphic source rocks which were chiefly metapelitic with a metamorphic overprint at amphibolite-facies conditions during Early Carboniferous. Another conceivable source for detrital rutile grains could be syn- to post-tectonic Carboniferous granites, mesothermal gold deposits and granite–pegmatite-hosted W–Sn mineralization owing to high elevated Sn and W concentrations in detrital rutile grains.
- The metapelitic and metamafic source lithologies are represented by Variscan amphibolite-facies metamorphic basement rocks that are present in the Sakarya Zone, Strandja Massif, Rhodope Massif. The Early Carboniferous amphibolite-facies metamorphism from the Sakarya Zone to the Caucasus occurred between 318 Ma and 340 Ma. The age of amphibolite-facies metamorphic rocks and P–T conditions suggest that the metamorphic massifs could be the primary source rocks for the detrital rutiles in the sandstones of the Jurassic Bayırköy Formation.

Acknowledgments: This study was supported by the Scientific and Technological Research Council of Turkey (TÜBİTAK) grant 124Y293 and the Scientific Research Coordination Unit of Çanakkale Onsekiz Mart University under the project number FBA-2023-4284.

References

Akyürek B., Duru M., Sütçü Y.F., Papak İ., Şaroğlu F., Pehlivan N., Gönenç O., Granit S. & Yaşar T. 1996: *Ankara ilinin çevre jeolojisi ve doğal kaynaklar projesi*. MTA Report. No: 9961.

Altıner D., Koçyiğit A., Farinacci A., Nicosia U. & Conti M.A. 1991: Jurassic, Lower Cretaceous stratigraphy and paleogeographic evolution of the southern part of north-western Anatolia. *Geological Romana* 28, 13–80.

Altınlı İ.E. 1973: *The Geology of middle Sakarya*. Congress Proceeding Earth Sciences 50th Anniversary of Turkish Republic. Mineral Research Exploration Institute (MTA), Ankara, 159–191 (in Turkish with English abstract).

Andersen T., Van Niekerk H. & Elburg M.A. 2022: Detrital Zircon in an Active Sedimentary Recycling System: Challenging the 'Source-to-sink' Approach to Zircon-based Provenance Analysis. *Sedimentology* 69, 2436–2462. https://doi.org/10.1111/sed.12996

Avigad D., Morag N., Abbo A. & Gerdes A. 2017: Detrital rutile U–Pb perspective on the origin of the great Cambro–Ordovician sandstone of North Gondwana and its linkage to orogeny. *Gondwana Research* 51, 17–29. https://doi.org/10.1016/j.gr.2017.07.001

Aygül M., Topuz G., Okay A.I., Satır M. & Meyer H.P. 2012: The Kemer Metamorphic Complex (NW Turkey), a subducted continental margin of the Sakarya Zone. *Turkish Journal of Earth Sciences* 21, 19–35. https://doi.org/10.3906/yer-1006-14

Aysal N., Ustaömer T., Öngen S., Keskin, M. Köksal S., Peytcheva I. & Fanning M. 2012a: Origin of the Early-Middle Devonian Magmatism in the Sakarya Zone, NW Turkey: Geochronology, Geochemistry and Isotope Systematics. *Journal of Asian Earth Science* 45, 201–222. https://doi.org/10.3906/10.1016/J.JSEAES.2011.10.011

Aysal N., Öngen S., Peytcheva I. & Keskin M. 2012b: Origin and evolution of the Havran Unit, Western Sakarya basement (NW Turkey): new LA-ICP-MS U-Pb dating of the metasedimentary-metagranitic rocks and possible affiliation to Avalonian microcontinent. *Geodinamica Acta* 25, 226–247. https://doi.org/10.1080/09853111.2014.882536

Barth M.G., McDonough W.F. & Rudnick R.L. 2000: Tracking the budget of Nb and Ta in the continental crust. *Chemical Geology* 165, 197–213. https://doi.org/10.1016/S0009-2541(99)00173-4

Carrigan C.W., Mukasa S.B., Haydoutov I. & Kolcheva K. 2006: Neoproterozoic magmatism and Carboniferous high-grademetamorphism in the Sredna Gora Zone: An extension of the Gondwana-derived Avalonian-Cadomian belt?. *Precambrian Research* 147, 404–416. https://doi.org/10.1016/j.precamres.2006.01.026

Che X.D., Linnen R.L., Wang R.C., Groat L.A. & Brand A.A. 2013: Distribution of trace and rare earth elements in titanite from tungsten and molybdenum deposits in Yukon and British Columbia. *Canadian Mineralogy* 51, 415–438. https://doi.org/10.3749/canmin.51.3.415

Chew D.M., Petrus J.A. & Kamber B.S. 2014: U–Pb LA–ICPMS dating using accessory mineral standards with variable common Pb. *Chemical Geology* 363, 185–199. https://doi.org/10.1016/j.chemgeo.2013.11.006

Chew D.M., O'Sullivan G., Caracciolo L., Mark C. & Tyrrell S. 2020: Sourcing the sand: accessory mineral fertility, analytical and other biases in detrital-provenance analysis. *Earth Science Reviews* 202, 103093. https://doi.org/10.1016/j.earscirev.2020.103093

Clark J.R. & Williams-Jones A.E. 2004: *Rutile as a potential indicator mineral for metamorphosed metallic ore deposits*. Rapport Final de DIVEX, Sous-project SC2, Montréal, Canada, 1–17.

Ding X., Lundstrom C., Huang F., Li J., Zhang Z.M., Sun X.M., Liang J.L. & Sun W.D. 2009: Natural and experimental constraints on formation of the continental crust based on niobium–tantalum fractionation. *International Geology Review* 51, 473–501. https://doi.org/10.1080/00206810902759749

Erdoğan B., Akay E., Hasözbek A., Satır M. & Siebel W. 2013: Stratigraphy and tectonic evolution of the Kazdağ Massif (NW Anatolia) based on field studies and radiometric ages. International Geology Review 55, 2060-2082. https://doi.org/10.1080/00206814.2013.818756

Ershova V., Prokopiev A. & Stockli D. 2024: Provenance of Detrital Rutiles from the Triassic–Jurassic Sandstones in Franz Josef Land (Barents Sea Region, Russian High Arctic): U–Pb Ages and Trace Element Geochemistry. *Geosciences* 14, 41. https://doi.org/10.3390/geosciences14020041

Foley S.F., Barth M.G. & Jenner G.A. 2000: Rutile/melt partition coefficients for trace elements and assessment of the influence of rutile on the trace element characteristics of subduction zone magmas. *Geochimica et Cosmochimica Acta* 64, 933–938. https://doi.org/10.1016/S0016-7037(99)00355-5

Force E.R. 1980: The provenance of rutile. *Journal of Sedimentary Petrology* 50, 485–488.

Galloway W.E. & Hobday D.K. 1983: *Terrigenous Clastic Depositional Systems*. Springer, New York, NY, USA.

Gamkrelidze I., Shengelia D., Tsutsunava T., Chung S.L., Yichiu H. & Chikhelidze K. 2011: New data on the U–Pb zircon age of the pre-alpine crystalline basement of the Black-Sea-Central Transcaucasian terrane and their geological significance. *Bulletin of the Georgian National Academy of Sciences* 5, 64–76.

Jamil M., Siddiqui N.A., Ahmed N., Usman M., Umar M., Rahim H.U. & Imran Q.S. 2021: Facies Analysis and Sedimentary Architecture of Hybrid Event Beds in Submarine Lobes: Insights from the Crocker Fan, NW Borneo, Malaysia. *Journal of Marine Science and Engineering* 9, 1133. https://doi.org/10.3390/jmse9101133

Jochum K.P., Nohl U., Herwig K., Lammel E., Stoll B. & Hofmann A.W. 2005: GeoReM: a new geochemical database for reference materials and isotopic standards. *Geostandards and Geoanalytical Research* 29: 333–338. https://doi.org/10.1111/j.1751-908X.2005.tb00904.x

Jochum K.P., Weis U., Stoll B., Kuzmin D., Yang Q., Raczek I., Jacob D.E., Stracke A., Birbaum K., Frick D.A., Günther D. & Enzweiler J. 2011: Determination of Reference Values for NIST SRM 610-617 Glasses Following ISO Guidelines. *Geostandards and Geoanalytical Research* 35, 397–429. https://doi.org/10.1111/j.1751-908X.2011.00120.x

Karslı O., Şengün F., Dokuz A., Kandemir R., Aydin F. & Andersen T. 2020: Silurian to Early Devonian arc magmatism in the western Sakarya Zone (NW Turkey), with inference to the closure of the Rheic Ocean. *Lithos* 370–371, 105641. https://doi.org/10.1016/j.lithos.2020.105641

Klemme S., Prowatke S., Hametner K. & Günther D. 2005: Partitioning of trace elements between rutile and silicate melts: Implications for subduction zones. *Geochimica et Cosmochimica Acta* 69, 2361–2371. https://doi.org/10.1016/j.gca.2004.11.015

Kohn M.J. 2020: A refined zirconium-in-rutile thermometer. *American Mineralogist* 105, 963–971. https://doi.org/10.2138/am-2020-7091

Kooijman E., Mezger K. & Berndt J. 2010: Constraints on the U–Pb systematics of metamorphic rutile from in situ LA-ICP-MS analysis. *Earth and Planetary Science Letters* 293, 321–330. https://doi.org/10.1016/j.epsl.2010.02.047

Kretz R. 1983: Symbols of rock-forming minerals. *American Mineralogist* 68, 27–279.

Liu L., Xiao Y., Wörner G., Kronz A., Simon K. & Hou Z. 2014: Detrital rutile geochemistry and thermometry from the Dabie orogen: Implications for source–sediment links in a UHPM terrane. *Journal of African Earth Sciences* 89, 123–140. https://doi.org/10.1016/j.jseaes.2014.04.003

Luvizotto G.L. & Zack T. 2009: Nb and Zr behavior in rutile during high-grade metamorphism and retrogression: an example from the Ivrea Verbano Zone. *Chemical Geology* 261, 303–317. https://doi.org/10.1016/j.chemgeo.2008.07.023

Machev P., Ganev V. & Klain L. 2015: New LA-ICP-MS U–Pb zircon dating for Strandja granites (SE Bulgaria): evidence for two-stage late Variscan magmatism in the internal Balkanides. *Turkish Journal of Earth Sciences* 24, 230–248. https://doi.org/10.3906/yer-1407-21

Mayringer F., Treloar J., Gerdes A., Finger F. & Shengelia D. 2011: New age data from the Dzirula Massif, Georgia: implications for the evolution of the Caucasian Variscides. *American Journal of Science* 311, 404–441. https://doi.org/10.2475/05.2011.02

Meinhold G. 2010: Rutile and its applications in earth sciences. *Earth Science Review* 102, 1–28. https://doi.org/10.1016/j.earscirev.2010.06.001

Meinhold G., Morton A.C., Fanning C.M. & Whitham A.G. 2011: U–Pb SHRIMP ages of detrital granulite-facies rutiles: further constraints on provenance of Jurassic sandstones on the Norwegian margin. *Geological Magazine* 148, 473–480. https://doi.org/10.1017/S0016756810000877

Miller C., Zanetti A. & Thoni M. 2007: Eclogitisation of gabbroic rocks: Redistribution of trace elements and Zr in rutile thermometry in an Eo-Alpine subduction zone (Eastern Alps). *Chemical Geology* 239, 96–123. https://doi.org/10.1016/j.chemgeo.2007.01.001

Moix P., Beccaletto L., Kozur H., Hochard C., Rosselet F. & Stampfli G.M. 2008: A new classification of the Turkish terranes and sutures and its implication for the paleotectonic history of the region. *Tectonophysics* 451, 7–39. https://doi.org/10.1016/j.tecto.2007.11.044

Morton A.C. & Hallsworth C. 1994: Identifying provenance-specific features of detrital heavy mineral assemblages in sandstones. *Sedimentary Geology* 90, 241–256. https://doi.org/10.1016/0037-0738(94)90041-8

Münker C., Pfänder J.A., Weyer S., Büchl A., Kleine T. & Mezger K. 2003: Evolution of planetary cores and the Earth–Moon system from Nb/Ta systematic. *Science* 301, 84–87. https://doi.org/10.1126/science.1084662

Natal'in B.A. Sunal G., Gün E., Wang B. & Zhiqing Y. 2016: Precambrian to Early Cretaceous rocks of the Strandja Massif (northwestern Turkey): evolution of a long-lasting magmatic arc. *Canadian Journal of Earth Sciences* 53, 1312–1335. https://doi.org/10.1139/cjes-2016-0026

Okay A.İ. & Göncüoğlu M.C. 2004: The Karakaya Complex: A Review of Data and Concepts. *Turkish Journal of Earth Science* 13, 77–95.

Okay A.İ. & Monié P. 1997: Early Mesozoic subduction in the Eastern Mediterranean: Evidence from Triassic eclogite in northwest Turkey. *Geology* 25, 595–598. https://doi.org/10.1130/0091-7613(1997)025<0595:EMSITE>2.3.CO;2

Okay A.İ. & Nikishin A.M. 2015: Tectonic evolution of the southern margin of Laurasia in the Black Sea region. *International Geology Review* 57, 1051–1076. https://doi.org/10.1080/00206814.2015.1010609

Okay A.İ. & Satır M. 2000a: Coeval plutonism and metamorphism in a latest Oligocene metamorphic core complex in Northwest Turkey. *Geological Magazine* 137, 495–516. https://doi.org/10.1017/S0016756800004532

Okay A.İ. & Satır M. 2000b: Upper Cretaceous Eclogite – Facies Metamorphic Rocks from the Biga Peninsula, Northwest Turkey. *Turkish Journal of Earth Science* 9, 47–56.

Okay A.I. & Topuz G. 2017: Variscan orogeny in the Black Sea region. *International Journal of Earth Science* 106, 569–592. https://doi.org/10.1007/s00531-016-1395-z

Okay A.İ. & Tüysüz O. 1999: Tethyan sutures of northern Turkey. In: Durand B., Jolivet L., Horváth F. & Séranne M. (Eds.): The Mediterranean Basins: Tertiary Extension within the Alpine Orogen. *Geological Society of London Special Publications* 156, 475–515. https://doi.org/10.1144/GSL.SP.1999.156.01.22

Okay A.İ., Siyako M. & Bürkan K.A. 1991: Geology and tectonic evolution of the Biga Peninsula. *Bulletin of the Technical University of Istanbul* 44, 191–255.

Okay A.İ., Satır M., Maluski H., Siyako M., Monie P., Metzger R. & Akyüz S. 1996: Paleo-and Neotethyan events in northwest Turkey. In: Yin A. & Harrison M. (Eds.): *Tectonics of Asia*. Cambridge University Press, 420–441.

Okay A.İ. Satır M., Tüysüz O., Akyüz S. & Chen F. 2001: The tectonics of the Strandja Massif: Late-Variscan and mid Mesozoic deformation and metamorphism in the northern Aegean. *International Journal of Earth Sciences* 90, 217–233. https://doi.org/10.1007/s005310000104

Okay A.İ., Monod O. & Monie P. 2002: Triassic blueschists and eclogites from northwest Turkey: Vestiges of the Paleo-Tethyan subduction. *Lithos* 64, 155–178. https://doi.org/10.1016/S0024-4937(02)00200-1

Okay A.İ., Satır M. & Siebel W. 2006: Pre-Alpide and Mesozoic orogenic events in the Eastern Mediterranean region. *Geological Society of London Memoirs* 32, 389–405. https://doi.org/10.1144/GSL.MEM.2006.032.01.23

Okay N., Zack T., Okay A.İ. & Barth M. 2011: Sinistral Transport Along the Trans-European Suture Zone: Detrital Zircon–Rutile Geochronology and Sandstone Petrography from The Carboniferous flysch Of the Pontides. *Geological Magazine* 148, 380–403. https://doi.org/10.1017/S0016756810000804

Paton C., Hellstrom J., Paul B., Woodhead J. & Hergt J. 2011: Iolite: freeware for the visualisation and processing of mass spectrometric data. *Journal of Analytical Atomic Spectrometry* 26, 2508–2518. https://doi.org/10.1039/C1JA10172B

Pereira I. & Storey C.D. 2023: Detrital rutile: Records of the deep crust, ores and fluids. *Lithos* 438–439, 107010. https://doi.org/10.1016/j.lithos.2022.107010

Pereira I., Storey C., Darling J., Lana C. & Alkmim A.R. 2019: Two billion years of evolution enclosed in hydrothermal rutile: Recycling of the São Francisco Craton Crust and constraints on gold remobilisation processes. *Gondwana Research* 68, 69–92. https://doi.org/10.1016/j.gr.2018.11.008

Pereira I. & Storey C.D., Strachan R.A. Bento dos Santos T. & Darling J.R. 2020: Detrital rutile ages can deduce the tectonic setting of sedimentary basins. *Earth and Planetary Science Letters* 537, 116193. https://doi.org/10.1016/j.epsl.2020.116193

Pereira I. & Storey C.D., Darling J.R., Moreira H., Strachan R.A. & Cawood P.A. 2021: Detrital rutile tracks the first appearance of subduction zone low T/P paired metamorphism in the Palaeoproterozoic. *Earth and Planetary Science Letters* 570, 117069. https://doi.org/10.1016/j.epsl.2021.117069

Pettijohn F.J. Potter P.E. & Siever R. 1987: *Sand and Sandstone*. Springer, New York, NY, USA.

Rice C.M., Darke K.E., Still J.W. & Lachowski E.E. 1998: Tungsten-bearing rutile from the Kori Kollo gold mine. Bolivia. *Mineralogical Magazine* 62, 421–429. https://doi.org/10.1180/002646198547684

Rösel D., Zack T. & Möller A. 2019: Interpretation and significance of combined trace element and U–Pb isotopic data of detrital rutile: a case study from late Ordovician sedimentary rocks of Saxo-Thuringia, Germany. *International Journal of Earth Sciences* 108, 1–25. https://doi.org/10.1007/s00531-018-1643-5

Rösel D., Schulze M.C., Wilmsen M., Zieger-Hofmann M., Linnemann U. & Mertz-Kraus R. 2025: LA-ICP-MS U–Pb dating and trace element analyses of detrital rutile from the Elbtal Group (Saxony, Germany): provenance constraints of the Saxonian Cretaceous Basin. *International Journal of Earth Sciences* 114, 1–21. https://doi.org/10.1007/s00531-024-02466-y

Rudnick R.L., Barth M., Horn I. & McDonough W.F. 2000: Rutile-bearing refractory eclogites: missing link between continents and depleted mantle. *Science* 287, 278–281. https://doi.org/10.1126/science.287.5451.278

Schönig J., von Eynatten H., Meinhold G. & Lünsdorf N.K. 2022: The sedimentary record of ultrahigh-pressure metamorphism: a perspective review. *Earth Science Reviews* 227, 103985. https://doi.org/10.1016/j.sedgeo.2018.07.009

Scott K.M. 2005: Rutile geochemistry as a guide to porphyry Cu–Au mineralization, Northparkes, New South Wales, Australia. *Geochemistry Exploration Environment Analysis* 5, 247–253. https://doi.org/10.1144/1467-7873/03-055

Şengör A.M.C. & Yılmaz Y. 1981: Tethyan evolution of Turkey: a plate tectonic approach. *Tectonophysics* 75, 181–241.

Şengün F. & Koralay O.E. 2017: Early Variscan magmatism along the southern margin of Laurasia: Geochemical and geochronological evidence from the Biga Peninsula, NW Turkey. *International Journal of Earth Sciences* 106, 811–826. https://doi.org/10.1007/s00531-016-1334-z

Şengün F. & Koralay O.E. 2019: Petrography, geochemistry and provenance of Jurassic sandstones from the Sakarya Zone, NW Turkey. *Turkish Journal of Earth Sciences* 28, 603–622. https://doi.org/10.3906/yer-1901-10

Şengün F. & Zack T. 2016: Trace element composition of rutile and Zr-in-rutile thermometry in meta-ophiolitic rocks from the Kazdağ Massif, NW Turkey. *Mineralogy and Petrology* 110, 547–560. https://doi.org/10.1007/s00710-016-0433-7

Şengün F., Yigitbas E. & Tunç İ.O. 2011: Geology and Tectonic Emplacement of Eclogite and Blueschist, Biga Peninsula, Northwest Turkey. *Turkish Journal of Earth Science* 20, 273–285. https://doi.org/10.3906/yer-0912-75

Şengün F., Zack T. & Dunkl I. 2020a: Provenance of detrital rutiles from the Jurassic sandstones in the Central Sakarya Zone, NW Turkey: U–Pb ages and trace element geochemistry. *Geochemistry* 80, 125667. https://doi.org/10.1016/j.chemer.2020.125667

Şengün F., Koralay O.E. & Kristoffersen M. 2020b: Zircon U–Pb age and Hf isotopic composition of the Carboniferous Gönen granitoid in the western Sakarya Zone of Turkey. *Turkish Journal of Earth Science* 29, 617–628. https://doi.org/10.3906/yer-1910-7

Shi Y.R., Liu D.Y., Kröner A., Jian P., Miao L.C. & Zhang F.Q. 2012: Ca. 1318 Ma A-type granite on the northern margin of the North China Craton: implications for intraplate extension of the Columbia supercontinent. *Lithos* 148, 1–9. https://doi.org/10.1016/J.LITHOS.2012.05.023

Stacey J.S. & Kramers J.D. 1975: Approximation of terrestrial lead isotope evolution by a two-stage model. *Earth and Planetary Science Letters* 26, 207– 221. https://doi.org/10.1016/0012-821X(75)90088-6

Sunal G. 2012: Devonian magmatism in the western Sakarya Zone, Karacabey Region, NW Turkey. *Geodinamica Acta* 25, 183–201. https://doi.org/10.1080/09853111.2013.858947

Tomkins H.S., Powell R. & Ellis D.J. 2007: The pressure dependence of the zirconium-in-rutile thermometer. *Journal of Metamorphic Geology* 25, 703–713. https://doi.org/10.1111/j.1525-1314.2007.00724.x

Topuz G. & Altherr R. 2004: Pervasive rehydration of granulites during exhumation – an example from the Pulur complex, Eastern Pontides, Turkey. *Mineralogy and Petrology* 81, 165–185. https://doi.org/10.1007/s00710-003-0034-0

Topuz G., Altherr R., Kalt A., Satır M., Werner O. & Schwarz W.H. 2004: Aluminous granulites from the Pulur complex, NE Turkey: a case of partial melting, efficient melt extraction and crystallization. *Lithos* 72, 183–207. https://doi.org/10.1016/j.lithos.2003.10.002

Topuz G., Altherr R., Schwarz W.H., Dokuz A. & Meyer H. 2007: Variscan Amphibolite-facies Rocks from the Kurtoğlu Metamorphic Complex (Gümüşhane Area, Eastern Pontides, Turkey). *International Journal of Earth Sciences* 96, 861–873. https://doi.org/10.1007/s00531-006-0138-y

Topuz G., Altherr R., Siebel W., Schwarz W.H., Zack T., Hasözbek A., Barth M., Satır M. & Şen C. 2010: Carboniferous high-potassium I-type granitoid magmatism in the Eastern Pontides: the Gümüşhane pluton (NE Turkey). *Lithos* 116, 92–110. https://doi.org/10.1016/j.lithos.2010.01.003

Topuz G., Candan O., Okay A.I., von Quadt A., Othman M., Zack T. & Wang J. 2020: Silurian anorogenic basic and acidic magmatism in Northwest Turkey: Implications for the opening of the Paleo-Tethys. *Lithos* 356–357, 105302. https://doi.org/10.1016/j.lithos.2019.105302

Triebold S., von Eynatten H. & Zack T. 2012: A recipe for the use of rutile in sedimentary provenance analysis. *Sedimentary Geology* 282, 268–275. https://doi.org/10.1016/j.sedgeo.2012.09.008

Uğurcan O.G., Ustaömer T. & Gerdes A. 2019: Cambrian-Early Ordovician Magmatism, Mid-Late Paleozoic Sedimentation and Early Carboniferous Metamorphism in the Central Sakarya Terrane; Sakarya Zone, NW Turkey. *International Earth Science Colloquium on the Aegean Region 2019 EASCA Izmir* 11.

Ustaömer P.A., Ustaömer T. & Robertson A.H.F. 2012: Ion Probe U–Pb Dating of the Central Sakarya Basement: A peri-Gondwana Terrane Intruded by late Lower Carboniferous Subduction/Collision-related Granitic Rocks. *Turkish Journal of Earth Science* 21, 905–932. https://doi.org/10.3906/yer-1103-1

Ustaömer T., Robertson A.H.R., Ustaömer P.A., Gerdes A. & Peytcheva I. 2013: Constraints on Variscan and Cimmerian magmatism and metamorphism in the Pontides (Yusufeli–Artvin area), NE Turkey from U–Pb dating and granite geochemistry. In: Robertson A.H.F., Parlak O., Ünlügenç U.C., (Eds.): Geological development of Anatolia and the easternmost Mediterranean region. *Geological Society of London* 372, 49–74. https://doi.org/10.1144/SP372.13

Vermeesch P. 2018: IsoplotR: a free and open toolbox for geochronology. *Geoscience Frontiers* 9, 1479–1493. https://doi.org/10.1016/j.gsf.2018.04.001

Vry J.K. & Baker J.A. 2006: LA–MC–ICPMS Pb–Pb dating of rutile from slowly cooled granulites. Confirmation of the high closure temperature for Pb diffusion in rutile. *Geochimica et Cosmochimica Acta* 70, 1807–1820. https://doi.org/10.1016/j.gca.2005.12.006

Yaşar I.D., Sayıt K., Miller B.V., Hames W.E., Koralay O.E., Jeong Y.J. & Göncüoğlu M.C. 2025: Multi-stage tectonic record of the Central Sakarya Terrane Basement (NW Turkey): Implications for the Paleozoic evolution of Rheic Ocean and northern Gondwanan margin. *GSA Bulletin* 137, 1649–1669. https://doi.org/10.1130/B37857.1

Yiğitbaş E., Şengün F. & Tunç İ.O. 2010: *Distribution and correlation of Mesozoic rock assemblages of NW Anatolia* (TÜBİTAK Report, Project No; ÇAYDAG 108Y232), 1–118 (in Turkish).

Zack T. & Kooijman E. 2017: Petrology and geochronology of rutile. Reviews in *Mineralogy and Geochemistry* 83, 443–467. https://doi.org/10.2138/rmg.2017.83.14

Zack T., Kronz A., Foley S.F. & Rivers T. 2002: Trace element abundances in rutiles from eclogites and associated garnet mica schists. *Chemical Geology* 184, 97–122. https://doi.org/10.1016/S0009-2541(01)00357-6

Zack T., Moraes R. & Kronz A. 2004: Temperature dependence of Zr in rutile. Empirical calibration of a rutile thermometer. *Contributions to Mineralogy and Petrology* 148, 471–488. https://doi.org/10.1007/s00410-004-0617-8

Zeh A., Cabral A.R., Koglin N. & Decker M. 2018: Rutile alteration and authigenic growth in metasandstones of the Moeda Formation, Minas Gerais, Brazil – a result of Transamazonian fluid–rock interaction. *Chemical Geology* 483, 397–409. https://doi.org/10.1016/j.chemgeo.2018.03.007

Electronic supplementary material is available online:
Supplementary Tables S1–S7 at https://geologicacarpathica.com/data/files/supplements/GC-77-4-Sengun_TablesS1-S7.xlsx